Published in final edited form as:
Acta Biomater. 2014 October ; 10(10): 4390–4399. doi:10.1016/j.actbio.2014.06.015.

Oxidized alginate hydrogels for BMP-2 delivery in long bone defects

Lauren B Priddy[a,b], **Ovijit Chaudhuri**[c], **Hazel Y Stevens**[d], **Laxminarayanan Krishnan**[a], **Brent A Uhrig**[a,d], **Nick J Willett**[a,d], and **Robert E Guldberg**[a,d]

[a]Parker H. Petit Institute for Bioengineering & Bioscience, Georgia Institute of Technology, 315 Ferst Drive NW, Atlanta, GA 30332, USA

[b]Wallace H. Coulter Department of Biomedical Engineering, Georgia Institute of Technology, 313 Ferst Drive NW, Atlanta, GA 30332, USA

[c]Department of Mechanical Engineering, Stanford University, 496 Lomita Mall, Stanford, CA 94305, USA

[d]George W. Woodruff School of Mechanical Engineering, Georgia Institute of Technology, 801 Ferst Drive NW, Atlanta, GA 30332, USA

Abstract

Autograft treatment of large bone defects and fracture non-unions is complicated by limited tissue availability and donor site morbidity. Polymeric biomaterials such as alginate hydrogels provide an attractive tissue engineering alternative due to their biocompatibility, injectability, and tunable degradation rates. Irradiated RGD-alginate hydrogels have been used to deliver proteins such as bone morphogenetic protein-2 (BMP-2), to promote bone regeneration and restoration of function in a critically sized rat femoral defect model. However, slow degradation of irradiated alginate hydrogels may impede integration and remodeling of the regenerated bone to its native architecture. Oxidation of alginate has been used to promote degradation of alginate matrices. The objective of this study was to evaluate the effects of alginate oxidation on BMP-2 release and bone regeneration. We hypothesized that oxidized-irradiated alginate hydrogels would elicit an accelerated release of BMP-2, but degrade faster *in vivo*, facilitating the formation of higher quality, more mature bone compared to irradiated alginate. Indeed, oxidation of irradiated alginate did accelerate *in vitro* BMP-2 release. Notably, the BMP-2 retained within both constructs was bioactive at 26 days, as observed by induction of alkaline phosphatase activity and positive Alizarin Red S staining of MC3T3-E1 cells. From the *in vivo* study, robust bone regeneration was observed in both groups through 12 weeks by radiography, micro-CT analyses, and biomechanical

Address correspondence to: Robert E. Guldberg, Ph.D., Parker H. Petit Institute for Bioengineering and Bioscience, Georgia Institute of Technology, 315 Ferst Drive, Atlanta, GA 30332-0363, USA, robert.guldberg@me.gatech.edu, Phone: +1 404 894 6589, Fax: +1 404 894 2291.

Disclosure Statement
No competing financial interests exist.

testing. Bone mineral density (BMD) was significantly greater for the oxidized-irradiated alginate group at 8 weeks. Histological analyses of bone defects revealed enhanced degradation of oxidized-irradiated alginate and suggested the presence of more mature bone after 12 weeks of healing.

Keywords

Bone regeneration; Alginate; BMP-2 (bone morphogenetic protein-2); Oxidation; Bioactivity

1. Introduction

Musculoskeletal injuries account for two-thirds of all injuries each year in the United States [1, 2]. Of the 6.3 million bone fractures that occur annually in the United States, over 500,000 require bone grafts, accounting for approximately $2.5 billion in medical expenses [3]. Substantial loss of bone tissue caused by traumatic injury or tumor resection presents a significant clinical challenge for reconstruction. Among these injuries, critically sized bone defects are particularly difficult to repair and often require subsequent surgeries or result in a non-union. Currently, the gold standard of care is autograft harvested from the iliac crest, but the limited graft tissue available and associated donor site pain and morbidity [4] warrant the study of more effective therapeutics.

Tissue engineering and regenerative medicine approaches, based on the delivery of osteoinductive cells, growth factors, and matrix materials, have emerged as a promising alternative platform. One clinically viable tissue engineering strategy is to deliver an osteogenic growth factor within a biomaterial scaffold to the site of injury and thereby stimulate the endogenous bone repair process [5]. A critical factor in the effectiveness of the carrier is the ability to provide the necessary temporal and spatial presentation of the growth factor for sufficient recruitment and differentiation of endogenous stem cells [5]. As members of the transforming growth factor-β (TGF-β) super family of growth factors, bone morphogenetic proteins (BMPs) promote migration of many cells including osteoprogenitors [6], and osteogenic differentiation of mesenchymal stem cells [7, 8]. Both BMP-2 and BMP-7 are approved by the FDA for clinical use [9, 10], and BMP-2 has been widely studied as an osteoinductive protein for bone regeneration. Although BMP-2 delivered on an absorbable collagen sponge has shown success in long bone healing and spinal fusion [11, 12], concerns regarding the use of supraphysiological doses and associated complications including heterotopic mineralization and inflammation [13] necessitate the development of biomaterial carriers that promote greater regenerative efficacy with lower doses of growth factors [14].

Alginate hydrogels have been used as delivery vehicles for a multitude of proteins, including BMP-2 [15-18]. Alginate is a polysaccharide derived from algae that exhibits minimal binding interactions with cells and can be ionically crosslinked into hydrogels using divalent cations such as calcium [19]. Alginate does not degrade enzymatically [18], but alginate hydrogels can degrade slowly due to dissociation of the ionic crosslinks [20]. Scaffold degradation is a crucial regulator of not only growth factor release but also extracellular

matrix deposition [21]. Ideally, as the scaffold degrades, space for new bone is created. As such, the rate of scaffold degradation should be similar to the rate of new tissue formation to allow for successful coalescence of the newly formed bone. In the case of alginate, various modification techniques, including gamma-irradiation and partial oxidation, have been utilized to enhance degradation of the scaffold [22-26].

Gamma-irradiation lowers the molecular weight of the alginate polymer chains, allowing the polymers to more readily dissociate from the alginate matrix [22]. Previously, irradiated alginate led to improved cellular infiltration and tissue healing compared to unmodified alginate [18, 22]. Irradiated alginate hydrogels have been used to deliver proteins such as BMP-2 and facilitate functional regeneration in our critically sized rat femoral segmental defect model [27-30]. In previous subcutaneous implant studies, irradiation of the alginate led to enhanced tissue infiltration, bone architecture, and bone area fraction [18, 22], as well as greater mineral density and extent of alginate degradation [22] compared to unmodified alginate.

Partial oxidation—whereby a small percentage of the uronate residues are oxidized—allows the polymer chains to be more susceptible to hydrolysis and increases the degradation rate *in vitro* [23-26]. Unlike the degradation of unmodified alginate, oxidized alginate breakdown occurs primarily via hydrolysis, specifically at the oxidized sugar residues [23]. Oxidation of the alginate creates a more open-chain structure while maintaining the ionic cross-linking capacity [24] and biocompatibility of the alginate [23]. In previous work, oxidized alginate hydrogels served as a carrier for chondrocytes [24] and growth factors (BMP-2 and TGF-β3) [25], and in both studies facilitated an increase in cellular infiltration and matrix formation subcutaneously compared to unmodified alginate. Additionally, oxidized alginate hydrogels loaded with vascular endothelial growth factor (VEGF) mitigated tissue loss in a mouse hind limb ischemia model [26]. Oxidized-irradiated alginate hydrogels were used recently for adipose stem cell delivery, promoting the formation of new adipose tissue subcutaneously [31]. In the present study, we utilized this same alginate modified by both irradiation and oxidation—i.e., a lower molecular weight and hydrolytically degradable alginate—as a growth factor delivery system for bone tissue engineering in an orthotopic model.

In our rat segmental defect model, irradiated alginate hydrogel surrounded by a PCL nanofiber mesh provided a more sustained release of BMP-2 and augmented bone regeneration compared to the clinically-used collagen sponge [28, 29]. However, a portion of the alginate material was shown to persist at 30 weeks and may have hindered functional remodeling of the newly formed bone tissue [32]. The interplay between carrier degradation, growth factor availability, and tissue ingrowth remains poorly understood. With these design parameters in mind, this work evaluated the regenerative capacity of an oxidized-irradiated alginate hydrogel as a delivery vehicle for BMP-2 in a well-established rat long bone defect model. The objectives of the study were: (i) to compare BMP-2 release and bioactivity from irradiated alginate and oxidized-irradiated alginate, and (ii) to evaluate bone regeneration, alginate degradation, and quality of regenerated bone *in vivo* using these two alginate formulations. We hypothesized that the oxidized-irradiated alginate hydrogels would elicit an accelerated release of BMP-2, but degrade faster *in vivo*, facilitating the formation of higher quality, more mature bone.

2. Materials and Methods

2.1. Alginate hydrogel preparation

Sodium alginate rich in guluronic acid blocks (MVG alginate, FMC BioPolymer) was used for all experiments. A low molecular weight alginate formulation was made by treating MVG alginate with gamma-irradiation, reducing its molecular weight from ~250 kDa to ~50 kDa [26]. For preparation of the oxidized-irradiated alginate, irradiated alginate was exposed to sodium periodate, resulting in ~1% oxidation of the uronate residues and creating a hydrolytically labile polymer [24]. The alginates were functionalized with RGD peptide sequences (2 sequences per polymer chain) [22] to promote cell adhesion. Alginates were reconstituted in alpha-Minimum Essential Medium (αMEM, Gibco) and mixed with recombinant human BMP-2 (rhBMP-2, R&D Systems) in 0.1% rat serum albumin. Hydrogels (2% (w/v) alginate) were prepared by mixing the alginate+rhBMP-2 solution with calcium sulfate slurry (0.21 g/mL) at a ratio of 25:1 [29]. All hydrogels were incubated at room temperature for 30 minutes before further manipulation. Hydrogels used for *in vivo* delivery were stored at 4°C overnight.

2.2. Nanofiber mesh production

Nanofiber meshes were fabricated as previously described [29]. Briefly, poly(ε-caprolactone) (PCL) was dissolved in a 90:10 volume ratio of hexafluoro-2-propanol:dimethylformamide (Sigma-Aldrich) to a 12% (w/v) concentration. The solution (5 mL) was electrospun onto a static collector plate for 5-6 hours. Using a VLS3.50 laser cutter (Universal Laser Systems) and CorelDRAW software, PCL sheets were cut into 12×19-mm rectangles, each with 24 1-mm diameter perforations, and rolled to form tubes 4.5 mm in diameter and 12 mm in length. Meshes were sterilized by ethanol evaporation overnight, rinsed three times in phosphate buffered saline (PBS, Cellgro), and stored in PBS. The meshes used *in vivo* were transferred to αMEM approximately 12 hours before surgery.

2.3. rhBMP-2 release kinetics

To investigate the release kinetics of BMP-2, 2% (w/v) alginate hydrogels (n=8) containing 500 ng rhBMP-2 per 150 μL were injected into PCL nanofiber meshes and incubated at 37°C in 1 mL PBS, as previously described [29]. PBS was collected and replaced at 3 and 15 hours, and at 1, 2, 3, 5, 8, 14, and 26 days. The BMP-2 remaining in the constructs at 26 days was then eluted by rinsing vigorously with PBS. The BMP-2 not removed by PBS rinsing was eluted using 1 mL 0.1% sodium dodecyl sulfate (SDS) on a rocker plate for 1 hour. SDS was removed from solution by an SDS-Out™ Precipitation Kit (Thermo Scientific). The BMP-2 in solution was quantified using an enzyme-linked immunosorbent assay (ELISA, R&D Systems) according to the manufacturer's protocol.

Using least-squares nonlinear regression analysis (SigmaPlot 11.0), the data of BMP-2 retained in the constructs was fit to a three term exponential decay function of the form $y(t) = a * \exp^{-\lambda t} + c$, where y is the percentage of BMP-2 retained in the constructs at time t, λ is the decay constant, or rate of decay, a+c is the initial value of y (100% at t=0), and the function is asymptotic to y=c ($t \rightarrow \infty$).

2.4. Alkaline phosphatase induction assay

The bioactivity of released and retained BMP-2 was determined using an alkaline phosphatase (ALP) induction assay [33] (n=6–7). Mouse clonal pre-osteoblasts (MC3T3-E1s, American Type Culture Collection) were seeded in 96-well plates at a density of 62,500 cells/cm^2 and incubated at 37°C, 5% CO_2 in αMEM with 20% fetal bovine serum (FBS, Atlanta Biologicals) and 1% penicillin-streptomycin-L-glutamine (PSL, Invitrogen) for 6 hours. Media was then replaced with a 1:1 volume ratio (200 μL total) of: (i) αMEM with 2% FBS and 0.2% ascorbic acid 2-phosphate (AA2P); and (ii) PBS containing released BMP-2 collected at 3 and 15 hours, and 1, 2, 3, and 5 days—or PBS/SDS containing BMP-2 remaining in the constructs at 26 days (all samples in triplicate). As a positive control, 20 ng BMP-2 in PBS was used. Wells without BMP-2 served as a negative control. After 3 days of culture, MC3T3s were washed 3 times with Hank's Buffered Salt Solution (HBSS, Thermo Scientific), fixed in 2% paraformaldehyde in 0.1 M sodium phosphate buffer for 10 minutes, and washed 3 times with sodium phosphate buffer (pH 7.4) for 3 minutes. MC3T3s were incubated with 100 μL/well of 7.6 mM p-Nitrophenyl Phosphate (p-NPP) in 50 mM Tris/HCl (pH 10.3) for 10 minutes at 37°C. The reaction was terminated by the addition of 100 μL/well of 0.2 M NaOH, and the absorbance was read at 405 nm using a microplate spectrophotometer (PowerWave X5, Gen5 Software; Biotek Instruments, Inc.). Absorbance values were converted to ALP activity (nmol/hr) using the linear relationship between p-NP standards (0-800 nmol/mL) and absorbance. Subsequently, mineralization in the MC3T3 cultures was observed by staining with Alizarin Red S.

2.5. Surgical procedure

Bilateral critically sized femoral segmental defects were created in 13-week-old female SASCO Sprague-Dawley rats (Charles River Laboratory) as previously described [27, 30]. Briefly, a radiolucent polysulfone fixation plate was affixed to the femur for limb stabilization, and an 8-mm defect was created in the mid-diaphysis of the femur. The defect was enclosed with a PCL nanofiber mesh and treated with 2 μg rhBMP-2 in 150 μL of irradiated alginate hydrogel or oxidized-irradiated alginate hydrogel (n=8). It was determined previously that 2 μg of rhBMP-2 promoted consistent bridging of the defects [28]. Subcutaneous injection of slow-release buprenorphine (Wildlife Pharmaceuticals) was provided for analgesia before surgery. Animals were euthanized by CO_2 inhalation at 12 weeks post-surgery. All procedures were approved by the Georgia Institute of Technology Institutional Animal Care and Use Committee (IACUC).

2.6. Radiography and micro-computed tomography

Bone regeneration was assessed qualitatively via radiography (Faxitron MX-20 Digital, Faxitron X-ray Corp.) at 2, 4, 8, and 12 weeks post-operatively. New bone formation was quantified by micro-computed tomography (micro-CT; Viva-CT 40, Scanco Medical) at 4, 8, and 12 weeks after surgery. The bone defect regions were scanned at medium resolution with a 38.9 μm voxel size, a voltage of 55 kVp, and a current of 145 μA. The volume of interest (VOI) for evaluation comprised the central 168 slices, or about 6.4 mm of the 8-mm defect region. A global threshold of 408 mg hydroxyapatite/cm^3, corresponding to

approximately 50% of the density of the native cortical bone, was applied to segment bone tissue. Noise was suppressed using a Gaussian filter (sigma = 1.2, support = 1).

2.7. Biomechanical testing

Torsional tests to failure were performed on femora (n=5) after harvest at 12 weeks post-surgery as previously described [30]. Briefly, the fixation plate was removed, the surrounding soft tissue was excised, and the native bone ends were potted in Wood's metal (Alfa Aesar). Femora were displaced at 3° per second to failure (ELF 3200; Bose ElectroForce Systems Group). Maximum torque, toughness (energy to failure), and torsional stiffness (linear region of the torque-rotation curve) were calculated for each sample.

2.8. Histological analyses

Histology was conducted on femora at 12 weeks (n=3) to identify newly formed bone and residual alginate within the defect region. Upon harvesting, femora were fixed with 10% neutral buffered formalin for 48 hours and decalcified under gentle agitation in a formic acid solution (Cal-ExII, Fisher Scientific), which was changed three times per week for two weeks. After paraffin processing, 5-μm mid-sagittal sections were cut and stained with hematoxylin and eosin (H&E), Safranin O (for alginate) and Fast green (for tissue infiltration) [28], Masson's trichrome (for bone) [34, 35], or Picrosirius red (for lamellar bone) [34]. Safranin O stained sections viewed by bright field microscopy were used for area quantification of alginate. The carboxyl groups in the alginate polymer contribute to its negative charge, which allows for staining with Safranin O [36, 37]. Although Safranin O also stains cartilage, chondrocytes are easily distinguishable from densely stained, acellular alginate. Picrosirius red stained sections were used for highlighting organized, lamellar bone under polarized light. The highly organized collagen of the native bone ends appeared green/yellow, so these colors were used to select mature, lamellar bone within the defect region [34]. For three consecutive sections per sample, five low magnification (10×) images from comparable areas within the bone defect region were used for automated image analysis, for a total of 15 images per sample. The location of each image was determined using the nanofiber mesh (which bordered the defect on both sides) as a marker. Image locations were as follows: top left corner of defect, bottom right corner of defect, and three central images distributed equally along the vertical length of the defect.

A custom MATLAB script (MATLAB 7.11.0 (R2010b)) was employed for automated and unbiased measurements on 10× magnification images (15 per sample, n=3) of de-identified sections. For images from Safranin O stained sections, areas of alginate (red), tissue (blue), and background (white) were identified by converting the images to HSV (Hue, Saturation, Value) color space [38]. The indices of the color areas were used to create a binary representation from which the areas of the image occupied by the red stained alginate, blue stained bone and fibrous tissue, and white backgrounds were estimated. For analysis of each image, red alginate areas were calculated as percentages of total area and binned from 0 - 100%. Alginate pieces constituting less than 1% of the total stained area were considered noise and excluded from analysis. This representation provided a comparison of the relative sizes of the residual alginate aggregates and served as a measure of alginate breakdown/fragmentation.

Similarly, for Picrosirius red stained images, the white colored tissue loci were demarcated by converting the image to YUV (luma and chrominance) and HSV color spaces. Subsequently, the original image, converted to HSV space, was used to identify loci of green/yellow color. Binary representations were built to calculate the relative areas of the respective colors. Additionally, a 50-pixel connectivity size filter (1.6 pixels/μm) was used to identify the larger contiguous areas in the green/yellow area binary representation. Mature, lamellar bone (green/yellow) area was calculated as a percentage of total stained area for each image.

2.9. Statistical analyses

All data were analyzed in GraphPad Prism 5 (GraphPad Software, Inc.) and reported as mean ± standard error of the mean (SEM). Two-way repeated measures analysis of variance (ANOVA) was performed on cumulative BMP-2 release. Decay constant and BMP-2 recovered from the constructs at 26 days were analyzed via t-tests. ALP activity of cells treated with released BMP-2 was evaluated using two-way ANOVA, while ALP activity of cells treated with construct-bound BMP-2 was performed by one-way ANOVA. Micro-CT parameters were evaluated using two-way repeated measures ANOVAs. For each ANOVA, a Bonferroni post-hoc test for pairwise comparisons was performed. Paired t-tests were performed on biomechanical data to evaluate differences between the two alginate formulations, while comparison to intact femora required additional (unpaired) t-tests. Histomorphometry of alginate area and lamellar bone area were analyzed by t-tests. A p-value less than 0.05 was considered statistically significant.

3. Results

3.1. rhBMP-2 release kinetics

The release of BMP-2 from irradiated and oxidized-irradiated alginate hydrogels loaded with 500 ng BMP-2 was assessed over 26 days. An initial burst release of BMP-2 from both alginate types was observed (Fig. 1A). Cumulative release was significantly greater for oxidized-irradiated alginate at days 2 and 3 ($p<0.05$). However, by day 5 these differences were no longer significant. Of the BMP-2 that was released (~20% of loaded), more than 95% was released by day 3 and day 8 for the oxidized-irradiated and irradiated alginates, respectively. The BMP-2 release data was also expressed as percent retained in the constructs through 26 days, and was fit to a three-term exponential decay function (Fig. 1B) to determine the decay constant, or rate of decay λ. The decay constant was significantly greater for the oxidized-irradiated alginate hydrogels ($p<0.05$) (Fig. 1C).

Approximately 35% of the loaded BMP-2 remained in the constructs at 26 days as measured by vigorous washing with PBS and SDS (Fig. 1D). A larger portion of the construct-bound BMP-2 was eluted during rinsing with PBS (~30% of loaded), as compared to the BMP-2 obtained from the SDS wash (~5% of loaded).

3.2. Alkaline phosphatase induction assay

Levels of ALP activity, an early marker of osteoblastic differentiation, were examined to evaluate the functional ability of the released BMP-2 to induce mineralization in MC3T3-E1

cells after 3 days of culture. ALP activity was significantly enhanced for cells treated with BMP-2 released through 1 day for the irradiated group and through 15 hours for the oxidized-irradiated group compared to the negative control (no BMP-2) ($p<0.05$) (Fig. 2A). BMP-2 released at 1 day from irradiated alginate elicited significantly higher ALP activity compared to the oxidized-irradiated group at that time point ($p<0.05$). ALP activities after day 1 were negligible. Although minimal BMP-2 was released after 8 days, BMP-2 remaining in both constructs at 26 days (obtained from PBS rinse) was bioactive, as indicated by ALP activity significantly greater than the negative control (Fig. 2B). Minimal ALP activity was measured by the subsequent SDS wash (data not shown). Alizarin Red S staining of calcium deposits in these same MC3T3 cultures treated with PBS/BMP-2 retained in the constructs at 26 days served as further evidence of BMP-2 bioactivity (Fig. 2C, D).

3.3. Radiography and micro-computed tomography

The *in vivo* comparison of bone regeneration with 2 μg BMP-2 in the two alginate formulations indicated similar, robust bone formation from radiographs and micro-CT. Radiographs at 2, 4, 8, and 12 weeks post-surgery revealed comparable bone formation for the irradiated alginate and oxidized-irradiated alginate groups (Fig. 3). For both groups, 7 of 8 defects showed bridging of the defect site by 4 weeks, and all 8 defects were bridged by 8 weeks, as is typical with this model and dose of BMP-2.

Micro-CT data at 4, 8, and 12 weeks post-surgery were consistent with the results from radiography. Bone volume increased over the course of the study for both groups but was not significantly different between the two groups at any time point (Fig. 4A). Bone mineral density (BMD) at 8 weeks was significantly greater in the oxidized-irradiated alginate group ($p<0.05$, Fig. 4B). The spatial distribution of BMD in a mid-sagittal slice within the defect region further demonstrated this difference at 8 weeks (Fig. 4C). By 12 weeks, however, these differences were no longer significant.

3.4. Biomechanical testing

Torsional testing to failure provided a measure of functional recovery of the newly regenerated bone at 12 weeks post-surgery. Data were also compared to historical data of age-matched, intact femora [29]. Maximum torque at failure was significantly attenuated in the irradiated alginate group compared to intact controls ($p<0.05$), while max torque for the oxidized-irradiated group was statistically equivalent to the irradiated group and control bone (Fig. 5A). Toughness, or area under the torque-rotation curve to failure, was not different between groups (Fig. 5B). Torsional stiffness was similar between groups and significantly greater than intact controls for both groups ($p<0.01$, Fig. 5C).

3.5. Histological analyses

Hematoxylin and eosin (H&E) staining of new bone (pink) and residual alginate (purple) showed distinct areas of bone and alginate in the irradiated group (Fig. 6A), and co-localization of bone and alginate in the oxidized-irradiated group (Fig. 6B). Masson's trichrome staining revealed bone tissue (red) within the defect region (Fig. 6C-D). The

presence of globular fatty cells and marrow-like structures observed with both stains was indicative of physiological bone regeneration.

Safranin O staining of the defect regions distinguished infiltrating bone tissue (blue) and residual alginate (red acellular areas) (Fig. 7A). Notably, no chondrocytes were present in the bone defect region. Although a considerable amount of both alginate types remained in the defect area, the oxidized-irradiated alginate was more diffuse and fragmented than the residual irradiated alginate. Histomorphometry was used to quantify residual alginate as a percentage of total image area. The number of alginate pieces comprising 1-10% area was greater for the oxidized-irradiated group. However, the average count of larger alginate pieces (>10% area) was significantly higher for the irradiated alginate group ($p<0.05$, Fig. 7B). Collectively, irradiated alginate occupied ~40% of total image area, while oxidized-irradiated alginate occupied ~30% (Fig. 7C).

Picrosirius red staining highlighted birefringent collagen under polarized light (Fig. 8A). While most of the collagen in the irradiated group was poorly organized woven bone, the oxidized-irradiated group appeared to contain more organized, lamellar bone (bright green/yellow). In both groups, woven bone (red) had formed in the available space created by degraded alginate and had integrated with the residual alginate. From histomorphometric analysis, lamellar bone area as a percentage of total stained area was statistically equivalent between groups (Fig. 8B).

4. Discussion

Irradiated alginate has previously been used to deliver BMP-2 in our critically sized rat bone defect model, facilitating enhanced bone regeneration over the clinically used collagen sponge [28, 39]. However, a portion of the alginate material remained in the defect beyond the typical 12-week time course of healing. Since bone tissue formation and remodeling may be impeded by the presence of residual biomaterial at the injury site, understanding the timelines of protein release and biomaterial degradation is crucial for complete restoration of the form and function of bone tissue. In introducing oxidation as an additional structural modification of the alginate, the goal was to maintain the appropriate functionality (e.g., biocompatibility and injectability) of the irradiated alginate, while accelerating alginate degradation to augment bone tissue formation and maturation. In this work, an oxidized-irradiated alginate hydrogel served as an effective carrier for BMP-2 in a critically sized segmental bone defect model, transiently improving mineral density of the bone tissue and enhancing alginate degradation at 12 weeks compared to a BMP-2-loaded irradiated alginate hydrogel.

In contrast to the relatively uncontrolled release of growth factors from unmodified, non-degradable alginate, which relies primarily on diffusion, growth factor release from irradiated and oxidized alginate hydrogels is accelerated by degradation of the alginate matrix [24]. Previous work has employed irradiation and oxidation as methods to modify alginate to allow for more tunable protein release kinetics, and the effects of varying the degree of alginate modification have been thoroughly examined [22, 23, 26]. In this work, the release of BMP-2 from oxidized-irradiated alginate was accelerated compared to that

from irradiated alginate, as measured by a larger decay constant (rate of release) for the oxidized-irradiated group. Others have observed a similar difference in release profiles of VEGF from oxidized-irradiated alginate compared to irradiated alginate [26]. However, the accelerated release (greater amount at early time points) of BMP-2 from oxidized-irradiated alginate did not translate to an increase in ALP activity for pre-osteoblasts *in vitro*. Furthermore, beyond day 1, ALP activity for BMP-2 released from both alginate types was negligible, suggesting that released BMP-2 did not maintain its bioactivity *in vitro*. ALP activity normalized to protein content revealed similar relationships between the groups (data not shown). The discrepancy between the ELISA and ALP results might be attributed to partial denaturation or misfolding of the protein once released, such that a portion of the BMP-2 was detected by ELISA but was not bioactive. Nonetheless, a burst release followed by minimal release of BMP-2 was observed from both alginates. Previously, *in vivo* BMP-2 release was tracked in our segmental defect model, and only ~10% of the protein remained at 21 days [28]. While Jeon et al. measured an increase in bone volume from a slow, sustained release of BMP-2 [40], others reported improved bone healing when an initial burst release was followed by a smaller sustained release [28, 41, 42].

Although minimal amounts of BMP-2 were released from both alginate types after one week (as seen previously with irradiated alginate [29]), approximately one-third of the loaded BMP-2 remained bound to the alginate/PCL nanofiber mesh constructs and was bioactive through 26 days. The bioactivity of the bound BMP-2 may have been prolonged due to retention of the protein within the constructs. Maintenance, and even possible enhancement, of bioactivity of VEGF, another heparin-binding growth factor, has been observed in the presence of alginate [26, 43]. Furthermore, BMP-2 bioactivity has been sustained on the order of weeks using various delivery vehicles, including PCL [44]. However, to our knowledge, this is the first demonstration of prolonged bioactivity of BMP-2 retained within alginate hydrogels, specifically an alginate/PCL mesh carrier. Likely, both the alginate hydrogel and the nanofiber mesh contributed to the binding of BMP-2, as BMP-2 retention was enhanced in the hybrid delivery system compared to both the mesh only and alginate only constructs (Fig. S1). However, the precise roles of each are yet to be delineated. The initial PBS wash removed most of the bound BMP-2, which we believe was loosely bound, while the remaining ~5% of loaded BMP-2 was eluted via SDS, which may have been bound more strongly to the mesh. An intermediate wash with sodium citrate (to dissolve the alginate) was performed, resulting in negligible amounts of BMP-2 measured. Alternatively, immediate hydrogel dissolution with sodium citrate at day 0 resulted in recovery of only ~200 ng of BMP-2 (data not shown), so a significant portion of BMP-2 seemed to be lost in the preparation of the hydrogels. In both cases, approximately half of the loaded BMP-2 was accounted for. It is possible that both the initial burst release and the localized retention of BMP-2 in the constructs facilitated bone regeneration, the former by recruiting the initial wave of osteoprogenitor cells to the defect site, and the latter by influencing the differentiation of osteoprogenitor cells once present within the defect space [42, 45]. Collectively, these findings suggest the bioavailability of BMP-2 for an extended time frame (~weeks) may be required for complete restoration of critically sized bone defects.

The degradation of hydrogels used in bone tissue engineering should ideally act in concert with the formation of new bone, so that by the completion of the regeneration process, only native bone fills the defect space. The increased degradation rate of oxidized alginate hydrogels compared to unmodified alginate hydrogels and irradiated alginate hydrogels has been characterized *in vitro* [23, 24, 26]. Qualitatively, the residual oxidized-irradiated alginate in the 12-week bone defect samples alginate appeared further degraded (less densely stained) than the irradiated alginate. Although no differences were observed in total alginate area, significantly fewer large fragments of oxidized-irradiated alginate were present. This difference in size distribution of residual alginate suggested that oxidation of irradiated alginate increased the degree of hydrolytic degradation. The more diffuse and fragmented oxidized-irradiated alginate may have allowed for an increase in cellular infiltration into the defect space, thereby promoting more rapid formation of organized, lamellar bone. Indeed, histomorphometry of lamellar bone area from Picrosirius red staining suggested a trend towards increased formation of lamellar bone in the oxidized-irradiated group. However, the multitude of factors contributing to the degradation of alginate *in vivo* makes understanding the role of each extremely difficult. In particular, a limitation of this work was the analysis of alginate degradation at a single time point (12 weeks); thus, the time course of alginate degradation in an orthotopic model remains unknown.

The breakdown of the oxidized-irradiated alginate may have been accelerated as the material degraded due to greater cellular invasion into the defect space. The well-understood role of the osteoprogenitor cells is two-fold: (i) secretion of cytokines to recruit additional mesenchymal stem cells and pre-osteoblasts, and (ii) differentiation and production of mineralized matrix, leading to the formation of bony tissue [46]. The cells' ability to deposit matrix relies on the concomitant degradation of the scaffold, creating space for and promoting consolidation of the newly formed bone tissue [22]. In this study, bone mineral density was significantly greater at 8 weeks in the oxidized-irradiated group. However, enhanced fragmentation of oxidized-irradiated alginate did not translate into augmented bone repair, as biomechanical function at 12 weeks was similar between groups. The limited degree of bone remodeling in the rat species and/or the small sample size may have hindered our ability to detect differences in this study, possibly leading to a type II error. Despite the lack of differences in bone healing, we observed robust bone regeneration with both alginate formulations, suggesting early release and local retention of BMP-2 may be an advantageous approach for growth factor delivery.

5. Conclusion

In conclusion, we observed prolonged bioactivity of BMP-2 at 26 days *in vitro* in both the irradiated and oxidized-irradiated alginate hydrogel/nanofiber mesh delivery systems. The oxidized-irradiated alginate hydrogel carrier for BMP-2 led to augmented mineral density, albeit temporarily, in a critically sized bone defect model. Furthermore, the residual oxidized-irradiated alginate was more diffuse and fragmented relative to the irradiated alginate at 12 weeks *in vivo*, although the hydrogels were not fully degraded at this time point. Thus, scaffold degradation remains a critical design parameter for evaluating the efficacy of growth factor delivery vehicles in tissue engineering.

Supplementary Material

Refer to Web version on PubMed Central for supplementary material.

Acknowledgments

This research was supported by the NIH T32EB006343 (Graduate Training for Rationally Designed, Integrative Biomaterials), NIH ARRA Grant R01 AR 056694, and Armed Forces Institute of Regenerative Medicine (AFIRM). The authors would like to thank Dr. Laura O'Farrell for veterinary assistance, Matthew Priddy for assistance with regression analyses, Dr. Brani Vidakovic for assistance with statistical methods, as well as Ashley Allen, Dr. Christopher Dosier, Mon-Tzu A. Li, Taran Lundgren, Tanushree Thote, and Jason Wang for assistance with surgeries.

References

[1]. Finkelstein, EA.; Corso, PS.; Miller, TR. Incidence and Economic Burden of Injuries in the United States. 1 ed. Oxford University Press; USA: 2006.

[2]. Praemer, A.; Furner, S.; Rice, DP. Musculoskeletal Conditions in the United States. 1 ed. Amer Acad of Orthopaedic Surgeons; 1999.

[3]. Laurencin C, Khan Y, El-Amin SF. Bone graft substitutes. Expert Rev Med Devices. 2006; 3:49–57. [PubMed: 16359252]

[4]. Sasso RC, LeHuec JC, Shaffrey C. Iliac crest bone graft donor site pain after anterior lumbar interbody fusion: a prospective patient satisfaction outcome assessment. J Spinal Disord Tech. 2005; 18:S77–81. [PubMed: 15699810]

[5]. Seeherman H, Wozney J, Li R. Bone morphogenetic protein delivery systems. Spine. 2002; 27:S16–23. [PubMed: 12205414]

[6]. Lind M, Eriksen EF, Bunger C. Bone morphogenetic protein-2 but not bone morphogenetic protein-4 and -6 stimulates chemotactic migration of human osteoblasts, human marrow osteoblasts, and U2-OS cells. Bone. 1996; 18:53–7. [PubMed: 8717537]

[7]. Wang EA, Israel DI, Kelly S, Luxenberg DP. Bone morphogenetic protein-2 causes commitment and differentiation in C3Hl0T1/2 and 3T3 cells. Growth Factors. 1993; 9:57–71. [PubMed: 8347351]

[8]. Wozney JM. The bone morphogenetic protein family and osteogenesis. Mol Reprod Dev. 2005; 32:160–7. [PubMed: 1637554]

[9]. Lieberman JR, Daluiski A, Einhorn TA. The role of growth factors in the repair of bone. J Bone Joint Surg. 2002; 84:1032–44. [PubMed: 12063342]

[10]. Nauth A, Ristevski B, Li R, Schemitsch EH. Growth factors and bone regeneration: how much bone can we expect? Injury. 2011; 42:574–9. [PubMed: 21489530]

[11]. Swiontkowski MF, Aro HT, Donell S, Esterhai JL, Goulet J, Jones A, et al. Recombinant human bone morphogenetic protein-2 in open tibial fractures. A subgroup analysis of data combined from two prospective randomized studies. J Bone Joint Surg. 2006:88. [PubMed: 16595451]

[12]. Cahill KS, Chi JH, Day A, Claus EB. Prevalence, complications, and hospital charges associated with use of bone-morphogenetic proteins in spinal fusion procedures. JAMA. 2009; 302:58–66. [PubMed: 19567440]

[13]. Shields LB, Raque GH, Glassman SD, Campbell M, Vitaz T, Harpring J, et al. Adverse effects associated with high-dose recombinant human bone morphogenetic protein-2 use in anterior cervical spine fusion. Spine. 2006; 31:542–7. [PubMed: 16508549]

[14]. Dickerman RD, Reynolds AS, Morgan BC, Tompkins J, Cattorini J, Bennett M. rh-BMP-2 can be used safely in the cervical spine: dose and containment are the keys! Spine J. 2007; 7:508–9. [PubMed: 17521966]

[15]. Augst AD, Kong HJ, Mooney DJ. Alginate hydrogels as biomaterials. Macromol Biosci. 2006; 6:623–33. [PubMed: 16881042]

[16]. Gombotz WR, Wee S. Protein release from alginate matrices. Adv Drug Delivery Rev. 1998; 31:267–85.

[17]. Lee KY, Peters MC, Anderson KW, Mooney DJ. Controlled growth factor release from synthetic extracellular matrices. Nature. 2000; 408:998–1000. [PubMed: 11140690]

[18]. Simmons CA, Alsberg E, Hsiong S, Kim WJ, Mooney DJ. Dual growth factor delivery and controlled scaffold degradation enhance in vivo bone formation by transplanted bone marrow stromal cells. Bone. 2004; 35:562–9. [PubMed: 15268909]

[19]. Rowley JA, Madlambayan G, Mooney DJ. Alginate hydrogels as synthetic extracellular matrix materials. Biomaterials. 1999; 20:45–53. [PubMed: 9916770]

[20]. Shoichet MS, Li RH, White ML, Winn SR. Stability of hydrogels used in cell encapsulation: an in vitro comparison of alginate and agarose. Biotechnol Bioeng. 1996; 50:374–81. [PubMed: 18626986]

[21]. Babensee JE, Anderson JM, McIntire LV, Mikos AG. Host response to tissue engineered devices. Adv Drug Delivery Rev. 1998; 33:111–39.

[22]. Alsberg E, Kong HJ, Hirano Y, Smith MK, Albeiruti A, Mooney DJ. Regulating bone formation via controlled scaffold degradation. J Dent Res. 2003; 82:903–8. [PubMed: 14578503]

[23]. Boontheekul T, Kong HJ, Mooney DJ. Controlling alginate gel degradation utilizing partial oxidation and bimodal molecular weight distribution. Biomaterials. 2005; 26:2455–65. [PubMed: 15585248]

[24]. Bouhadir KH, Lee KY, Damm KL, Anderson KW, Mooney DJ. Degradation of partially oxidized alginate and its potential application for tissue engineering. Biotechnol Prog. 2001; 17:945–50. E. A. [PubMed: 11587588]

[25]. Kong HJ, Kaigler D, Kim K, Mooney DJ. Controlling rigidity and degradation of alginate hydrogels via molecular weight distribution. Biomacromolecules. 2004; 5:1720–7. [PubMed: 15360280]

[26]. Silva EA, Mooney DJ. Spatiotemporal control of vascular endothelial growth factor delivery from injectable hydrogels enhances angiogenesis. J Thromb Haemost. 2007; 5:590–8. [PubMed: 17229044]

[27]. Boerckel JD, Dupont KM, Kolambkar YM, Lin AS, Guldberg RE. In vivo model for evaluating the effects of mechanical stimulation on tissue-engineered bone repair. Journal of biomechanical engineering. 2009; 131:084502. [PubMed: 19604025]

[28]. Boerckel JD, Kolambkar YM, Dupont KM, Uhrig BA, Phelps EA, Stevens HY, et al. Effects of protein dose and delivery system on BMP-mediated bone regeneration. Biomaterials. 2011; 32:5241–51. [PubMed: 21507479]

[29]. Kolambkar YM, Dupont KM, Boerckel JD, Huebsch N, Mooney DJ, Hutmacher DW, et al. An alginate-based hybrid system for growth factor delivery in the functional repair of large bone defects. Biomaterials. 2011; 32:65–74. [PubMed: 20864165]

[30]. Oest ME, Dupont KM, Kong HJ, Mooney DJ, Guldberg RE. Quantitative assessment of scaffold and growth factor-mediated repair of critically sized bone defects. Journal of orthopaedic research: official publication of the Orthopaedic Research Society. 2007; 25:941–50. [PubMed: 17415756]

[31]. Kim WS, Mooney DJ, Arany PR, Lee K, Huebsch N, Kim J. Adipose tissue engineering using injectable, oxidized alginate hydrogels. Tissue Eng A. 2012; 18:737–43.

[32]. Boerckel, JD. Mechanical Regulation of Bone Regeneration and Vascular Growth in vivo. Georgia Institute of Technology; 2011.

[33]. Wiemann M, Rumpf HM, Bingmann D, Jennissen HP. The binding of rhBMP-2 to the receptors of viable MC3T3-E1 cells and the question of cooperativity. Materialwiss Werkst. 2001; 32:931–6.

[34]. Patterson J, Siew R, Herring SW, Lin AS, Guldberg R, Stayton PS. Hyaluronic acid hydrogels with controlled degradation properties for oriented bone regeneration. Biomaterials. 2010; 31:6772–81. [PubMed: 20573393]

[35]. Zara JN, Siu RK, Zhang X, Shen J, Ngo R, Lee M, et al. High doses of bone morphogenetic protein 2 induce structurally abnormal bone and inflammation in vivo. Tissue Eng A. 2011; 17:1389–99.

[36]. Chubinskaya S, Huch K, Schulze M, Otten L, Aydelotte MB, Cole AA. Gene expression by human articular chondrocytes cultured in alginate beads. Journal of Histochemistry & Cytochemistry. 2001; 49:1211–9. [PubMed: 11561005]

[37]. You JO, Park SB, Park HY, Haam S, Chung CH, Kim WS. Preparation of regular sized Ca-alginate microspheres using membrane emulsification method. Journal of Microencapsulation. 2001; 18:521–32. [PubMed: 11428680]

[38]. How can I convert an RGB image to grayscale but keep one color?. http://stackoverflow.com/questions/4063965/how-can-i-convert-an-rgb-image-to-grayscale-but-keep-one-color

[39]. Kolambkar YM, Boerckel JD, Dupont KM, Bajin M, Huebsch N, Mooney DJ, et al. Spatiotemporal delivery of bone morphogenetic protein enhances functional repair of segmental bone defects. Bone. 2011; 49:485–92. [PubMed: 21621027]

[40]. Jeon O, Song SJ, Yang HS, Bhang SH, Kang SW, Sung MA, et al. Long-term delivery enhances in vivo osteogenic efficacy of bone morphogenetic protein-2 compared to short-term delivery. Biochemical and biophysical research communications. 2008; 369:774–80. [PubMed: 18313401]

[41]. Brown KV, Li B, Guda T, Perrien DS, Guelcher SA, Wenke JC. Improving bone formation in a rat femur segmental defect by controlling bone morphogenetic protein-2 release. Tissue Eng A. 2011; 17:1735–46.

[42]. Li B, Yoshii T, Hafeman AE, Nyman JS, Wenke JC, Guelcher SA. The effects of rhBMP-2 released from biodegradable polyurethane/microsphere composite scaffolds on new bone formation in rat femora. Biomaterials. 2009; 30:6768–79. [PubMed: 19762079]

[43]. Peters MC, Isenberg BC, Rowley JA, Mooney DJ. Release from alginate enhances the biological activity of vascular endothelial growth factor. J Biomater Sci, Polym Ed. 1998; 9:1267–78. [PubMed: 9860169]

[44]. Rai B, Teoh SH, Hutmacher DW, Cao T, Ho KH. Novel PCL-based honeycomb scaffolds as drug delivery systems for rhBMP-2. Biomaterials. 2005; 26:3739–48. [PubMed: 15621264]

[45]. Li RH, Wozney JM. Delivering on the promise of bone morphogenetic proteins. Trends Biotechnol. 2001; 19:255–65. [PubMed: 11412949]

[46]. Urist MR. Bone: Formation by Autoinduction. Science. 1965; 150:893–9. [PubMed: 5319761]

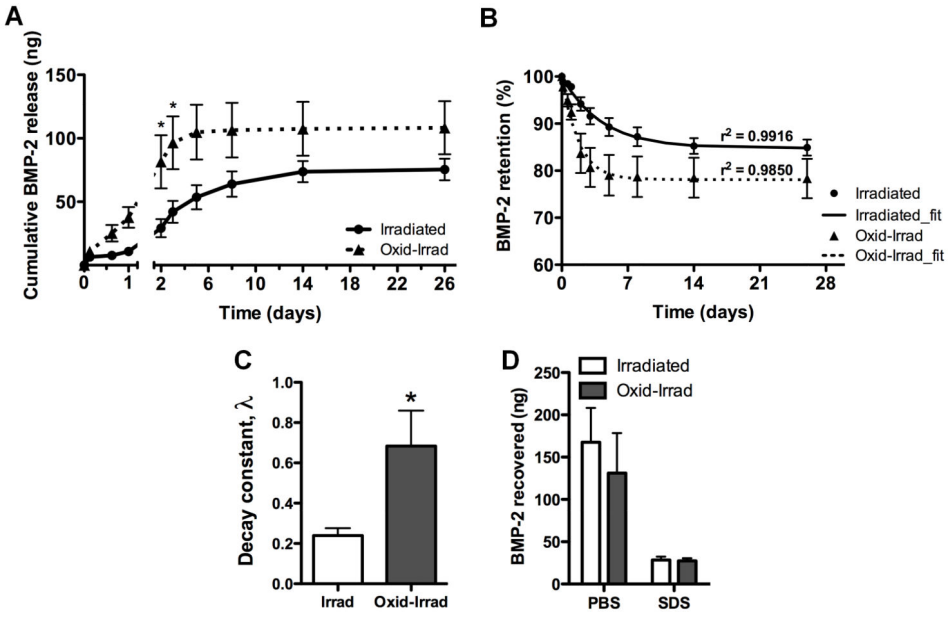

Figure 1.

(A) Release kinetics of BMP-2 from alginate gels. Significantly more BMP-2 had been released from oxidized-irradiated alginate at days 2 and 3 (*$p<0.05$). (B) Percentages of BMP-2 retained in the constructs over time were fit to exponential decay functions (denoted by _fit). (C) Decay constant λ was significantly greater for the oxidized-irradiated alginate (*$p<0.05$). (D) Approximately 35% of the BMP-2 was recovered from the constructs at 26 days.

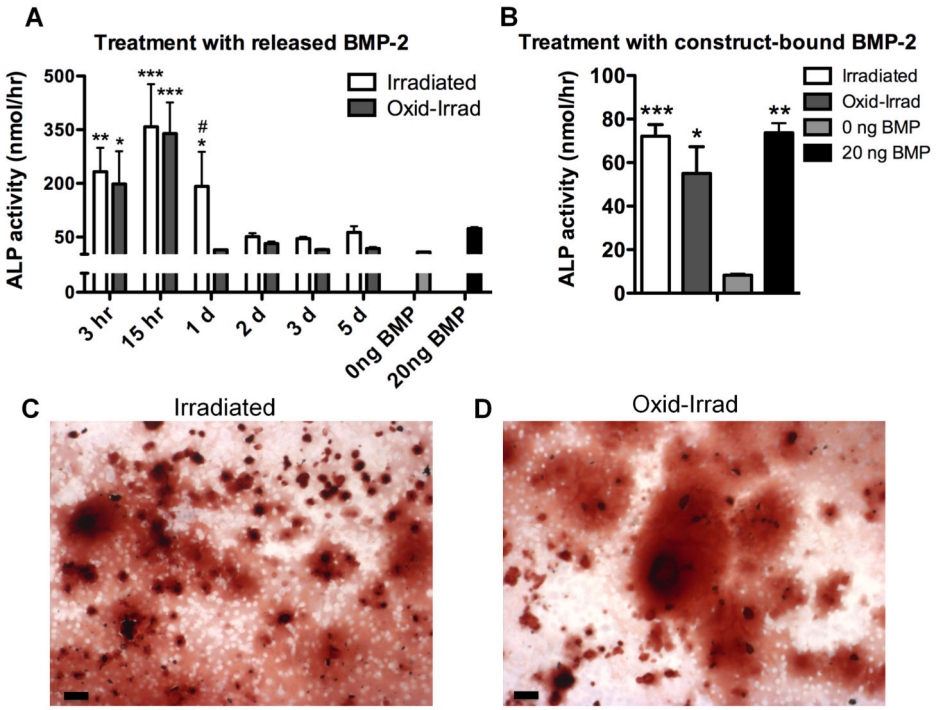

Figure 2.

(A) ALP activity was highest for MC3T3-E1 cells incubated with PBS/BMP-2 collected at 15 hr. Bioactivity of BMP-2 released from irradiated hydrogels through 1 day, and from oxidized-irradiated hydrogels through 15 hr, was significantly greater than the negative control (***$p<0.001$, **$p<0.01$, *$p<0.05$). BMP-2 released from irradiated alginate at 1 day showed significantly higher ALP activity than BMP-2 from oxidized-irradiated alginate at the same time point (#$p<0.05$). (B) BMP-2 remaining in the constructs at 26 days was bioactive, as all groups were significantly greater than the negative control. (C-D) Alizarin Red S staining of calcium deposits in MC3T3 cultures treated with BMP-2 retained in the constructs at 26 days. Scale bar = 100 μm.

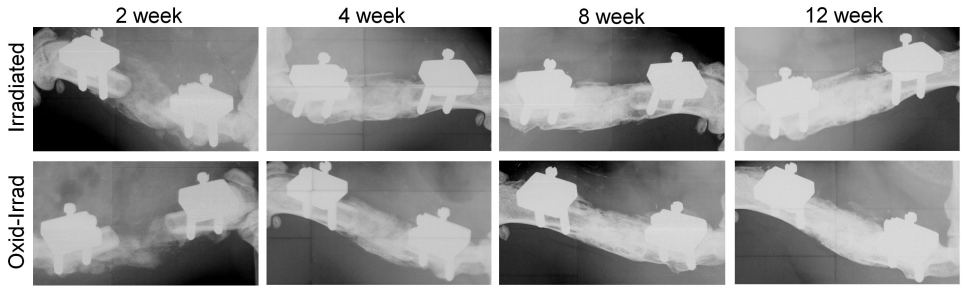

Figure 3.

Representative radiographs of defects treated with BMP-2 in irradiated alginate (top) or oxidized-irradiated alginate (bottom) at 2, 4, 8, and 12 weeks post-operatively. All defects showed complete bridging by 8 weeks.

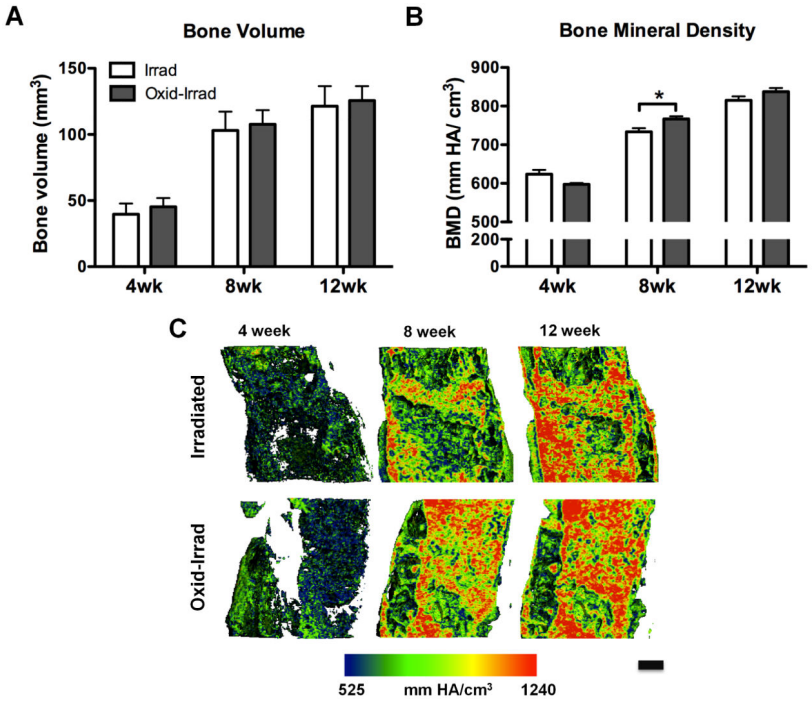

Figure 4.

(A) Bone volume increased over time, but no differences were observed between groups. (B) Bone mineral density (BMD) also increased over time for both groups and was significantly greater in the oxidized-irradiated alginate group at 8 weeks (*$p<0.05$). (C) Density mapping of mid-sagittal cross-sections of newly formed bone in the central defect region further illustrated this higher density at 8 weeks in the oxidized-irradiated alginate group. Scale bar = 1 mm.

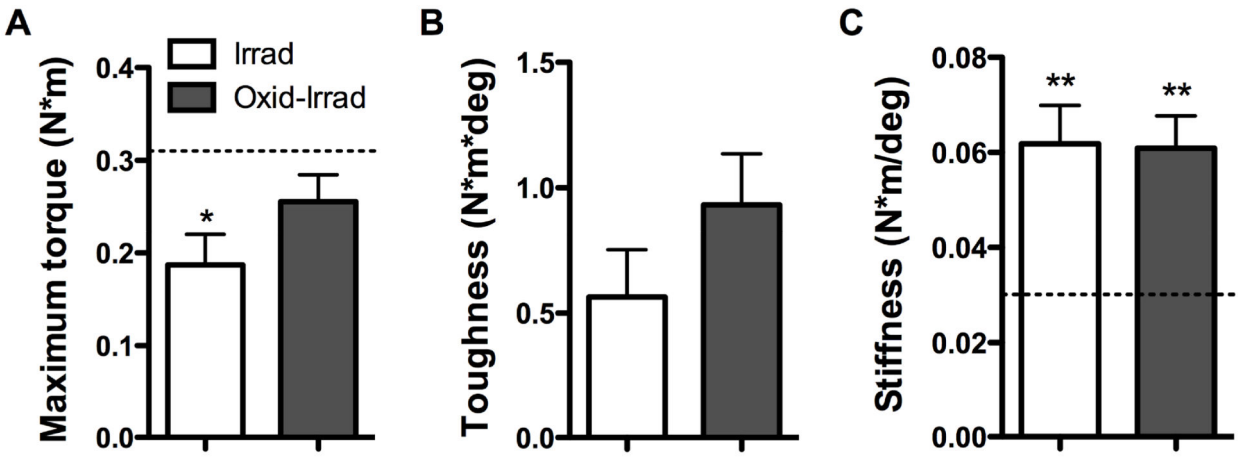

Figure 5.

Functional assessment of the regenerated bone at 12 weeks. Dashed lines indicate mean values for historical naïve intact control bone [25]. (A) Maximum torque to failure was not significantly different between test groups. However, max torque for the irradiated alginate group was significantly lower than intact controls (*$p<0.05$). (B) Toughness, or energy to failure. (C) Torsional stiffness for both groups was significantly greater than intact controls (**$p<0.01$).

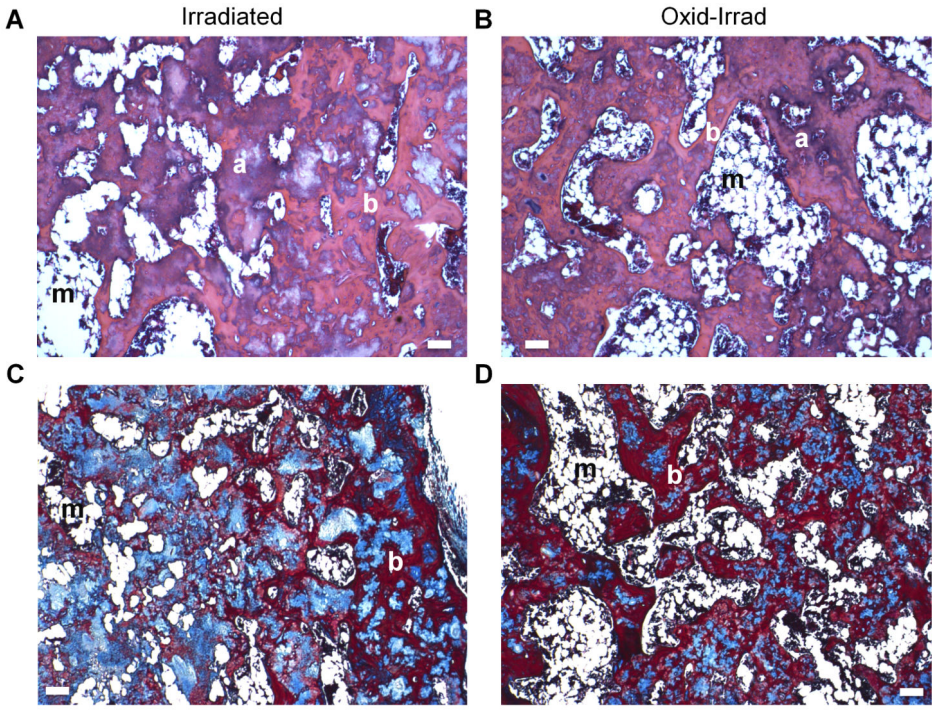

Figure 6.

12 week histology of mid-sagittal sections of bone defect tissue. (A, B) H&E staining revealed areas of new bone (pink, b) and residual alginate (purple, a), which appeared more interspersed/co-localized in the oxidized-irradiated group. (C, D) From Masson's trichrome staining, bone tissue stained red (b). (A-D) Globular, marrow-like structures (m) suggested physiological bone healing. Scale bar = 100 μm.

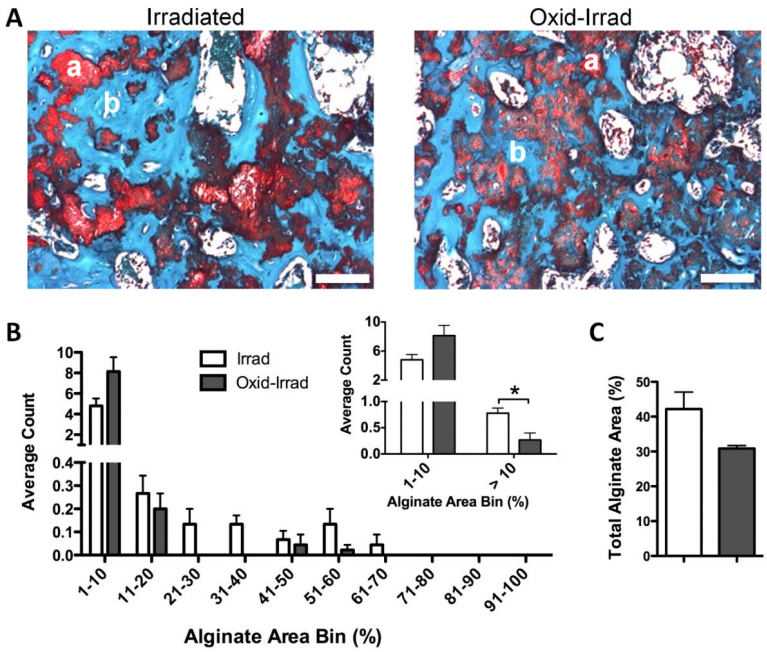

Figure 7.

Histomorphometry of alginate in 12 week bone defect samples. (A) Alginate stained red (a) and newly formed bone stained blue (b) with Safranin O. Residual oxidized-irradiated alginate was more diffuse and fragmented than irradiated alginate. (B) Frequency distribution of percent area of alginate pieces. Significantly more large (>10%) irradiated alginate pieces remained (*$p<0.05$). (C) Overall, irradiated alginate occupied ~40% of total area, while oxidized-irradiated comprised ~30%, although these differences were not statistically significant ($p=0.0831$). Scale bar = 100 μm.

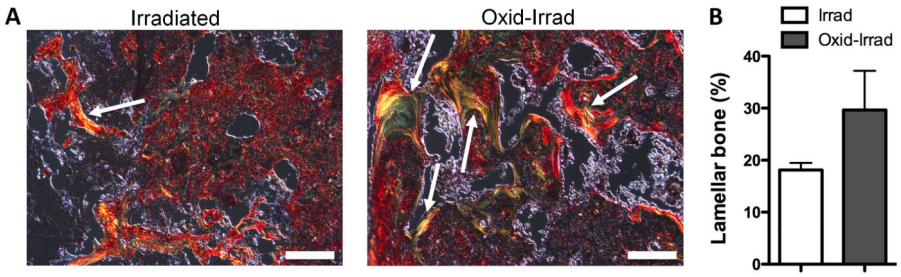

Figure 8.

Histomorphometry of lamellar bone in 12 week bone defect samples. (A) Picrosiruis red staining viewed under polarized light highlighted organized, lamellar bone (bright green/yellow, arrows), which appeared more abundant in the oxidized-irradiated alginate group. (B) Quantification of lamellar bone as a percentage of stained area. Scale bar = 100 μm.